Probing phase coexistence and stabilization of the spin-ordered ferrimagnetic state by calcium addition in the $Y(Ba_{1-x}Ca_x)Co_2O_{5.5}$ layered cobaltites using neutron diffraction

G. Aurelio,* J. Curiale,† and R. D. Sánchez‡
Comisión Nacional de Energía Atómica, Centro Atómico Bariloche, Avenida Bustillo 9500, 8400 S. C. de Bariloche, RN, Argentina

G. J. Cuello
Institut Laue Langevin, BP 156, F-38042 Grenoble Cedex 9, France

(Received 5 May 2007; revised manuscript received 19 July 2007; published 20 December 2007)

We study the effects of a partial substitution of Ba with the smaller cation Ca in the layered cobaltites $YBaCo_2O_{5+\delta}$ for $\delta \approx 0.5$. Neutron thermodiffractograms are reported for the compounds $YBa_{0.95}Ca_{0.05}Co_2O_{5.5}$ ($x_{Ca}=0.05$) and $YBa_{0.90}Ca_{0.10}Co_2O_{5.5}$ ($x_{Ca}=0.10$) in the temperature range 20 K$\leqslant T \leqslant$300 K, as well as high-resolution neutron diffraction experiments at selected temperatures for the samples $x_{Ca}=0.05$, $x_{Ca}=0.10$, and the parent compound $x_{Ca}=0$. We have found the magnetic properties to be strongly affected by the cationic substitution. Although the "122" perovskite structure seems unaffected by Ca addition, the magnetic arrangements of Co ions are drastically modified: the antiferromagnetic (AFM) long-range order is destroyed, and a ferrimagnetic phase with spin state order is stabilized below $T \sim 290$ K. For the sample with $x_{Ca}=0.05$ a fraction of AFM phase coexists with the ferrimagnetic one below $T \sim 190$ K, whereas for $x_{Ca}=0.10$ the AFM order is completely lost. The systematic refinement of the whole series has allowed for a better understanding of the observed low-temperature diffraction patterns of the parent compound $YBaCo_2O_{5.5}$, which had not yet been clarified. A two-phase scenario is proposed for the $x_{Ca}=0$ compound which is compatible with the phase coexistence observed in the $x_{Ca}=0.05$ sample.

DOI: 10.1103/PhysRevB.76.214417 PACS number(s): 75.25.+z, 61.12.Ld, 75.30.Kz, 61.66.Fn

I. INTRODUCTION

During the last decade, cobaltites have gained increased attention. A great effort is being made to clarify and systematize the extremely rich variety of phenomena they exhibit. Initially, they were expected to show similar properties to other perovskite-family members, such as manganites and cuprates,[1–5] but soon it was found that they present additional tunable features, as the cobalt spin state, that add to their complexity but also make them even more fascinating and challenging. Among cobaltites, the layered compounds $RBaCo_2O_{5+\delta}$ (R being a rare earth) are currently being intensively studied.[3–6] The oxygen content in these compounds can be modified in a wide range ($0 \leqslant \delta \leqslant 0.9$ depending on the R cation and the synthesis conditions),[6] which in turn controls the mixed valence state of Co ions. Several factors strongly influence the physical properties of these cobaltites: the nonstoichiometry, the R-cation size, the vacancies structural order, and—as we will show in the present work—also the structural disorder introduced by doping the Ba site with small quantities of smaller cations with the same valence state.

From a structural point of view, $RBaCo_2O_{5+\delta}$ is formed by a stacking sequence of $[CoO_2]$-$[BaO]$-$[CoO_2]$-$[RO_\delta]$ planes along the c axis,[2,7] the usually called "112" structure derived form the $a_P \times a_P \times 2a_P$ cell, a_P being the perovskite unit-cell constant. The symmetry may be tetragonal or orthorhombic, depending on the oxygen content and the R cation. The oxygen vacancies have a strong tendency to become ordered, which results in several superstructures.[8]

Of particular interest is the case $\delta=0.5$, for which Co is expected to be completely in the 3+ valence state. In this case, a particular order of oxygen vacancies leads to the "122" superstructure, consisting of an ordered array of 50% Co atoms in octahedral oxygen coordination and 50% in a pyramidal environment. This, in turn, favors a metal-insulator (MI) transition just above room temperature (the T_{MI} depends again on the R cation) which can be found only for δ values very close to 0.5.[4] When doping with holes (Co^{4+}, $\delta > 0.5$) these compounds behave as metals above the T_{MI} transition, but when doping with electrons (Co^{2+}, $\delta < 0.5$), these do not seem to participate in charge transport, which has been explained in terms of a spin blockade.[9] There has arisen a big controversy regarding the physical phenomena which occur at T_{MI}. Regardless of the R cation, cobaltites with $\delta \sim 0.5$ all show a jump in resistivity and a concomitant lattice distortion with a sudden volume collapse. The distortion is associated with specific changes in the Co-O distances in pyramids and octahedra, and became the subject of different interpretations. A possible driving force for the MI transition has been proposed to be a spin-state transition from the Co low-spin state (LS: $t_{2g}^6 e_g^0$) to a high-spin state (HS: $t_{2g}^4 e_g^2$) occurring only at the octahedral sites.[10] For the particular cases of R=Pr[11] and Gd,[10,12] this hypothesis would also be supported by a change in the slope of the inverse susceptibility curve at T_{MI}, which has been analyzed in terms of the Curie-Weiss model. Further support to this scenario was given by Maignan *et al.*[9] for R=Ho based on thermoelectric measurements, showing that the spin blockade mechanism is fully compatible with this picture. Other authors have proposed that a t_{2g}-e_g hybridization is enhanced in the metallic phase by the lattice distortion, such that the metallic or insulating behavior would be determined by the intersite mixing of the itinerant $3d$ electrons between the octahedral and pyramidal sites.[13] For R=Tb the distortions of pyramids and octahedra were interpreted as a $d_{3x^2-r^2}/d_{3y^2-r^2}$ orbital-

ordering transition accompanied by a intermediate-spin (IS: $t_{2g}^5 e_g^1$) to HS spin-state transition.[7] Furthermore, Pomjakushina *et al.*[14] proposed that the observed volume collapse at the transition temperature and the existence of an isotopic effect are indicative of a charge delocalization breaking the orbital order of the insulating phase, which could be compatible with a spin-state switch, but occurring in pyramids, not in octahedra. It seems obvious that this issue is far from being clarified and some effort must be made to systematize the study of the MI transition in cobaltites.

A second controversy, closely related to the one mentioned in the previous paragraph, concerns the low-temperature ordering of the magnetic moments at the Co sites. Again, the feature which seems to be common to all *R* cobaltites is the existence of a spontaneous magnetization in a more or less narrow temperature range, depending on *R*, below room temperature. Above this range they are paramagnetic, and below this range they transform to an antiferromagnetic (AFM) state. It is now well established that the origin of the spontaneous magnetization is not a ferromagnetic order, but among the two remaining possibilities—i.e., a ferrimagnetic phase or a canted AFM phase—there are various different models which have been proposed. Some of these models involve a so-called spin-state ordering (SSO) in which not only the spin state may be different between Co atoms located at pyramids and Co atoms located at octahedra, but also among the pyramidal[15] or the octahedral sites[16,17] a SSO may arise, leading to a doubling of the *a* axis in the unit cell. Indeed, a theoretical work by Khomskii and Löw[18] showed that such spin superstructures can be energetically favorable. These models would correspond to a ferrimagnetic phase. On the other hand, the proposers of canted-AFM models argue that there is no structural evidence for the doubling of the *a* axis and adopt the canted models which also explain the neutron diffraction data, with a doubling of the *a* axis just in the magnetic cell.[11,19] However, some care must be taken when comparing all these experimental data. For instance, there may be no evidence of a "222" superstructure in cobaltites with R=Gd and Pr,[11] but the case might be different for other lanthanides. In fact, some studies using NMR techniques showed that for R=Y, there are four nonequivalent Co sites at low temperature,[20] and for R=Eu, there are three,[21] which is compatible with the SSO scenario. It should be emphasized, too, that the "222" superstructure is very hard to detect from diffraction measurements unless an exceptionally high signal-to-noise ratio is attained. Using transmission geometry, Chernenkov *et al.*[22] have shown that the superstructure can indeed be observed in single crystals with R=Gd using x-ray diffraction. In all cases, there seems to be consensus on the IS character of pyramidal Co atoms,[5,10,23–25] although the spin state—or spin states—at octahedral sites remains uncertain or may, at least, depend on the *R* size.

Most studies of layered cobaltites were conducted for *R* among the lanthanides, but the compound with $R=Y^{3+}$, which is a small, nonmagnetic ion, is a good candidate to isolate the intrinsic properties of Co and explore the small-*R* region of the phase diagram. It is now well documented, for instance, that the MI transition temperature decreases with the *R* size. To gain more insight into the possible role of disorder we have introduced a second source of distortion by substituting the Ba site with Ca, which has a smaller atomic radius. In addition, it has recently been postulated on the basis of density-functional-theory calculations that a smaller cation substitution in the Ba site of small lanthanide cobaltites could be a promising compound to exhibit enhanced giant magnetoresistance properties.[26] The present work is aimed at characterizing and correlating the Ba-substituted compounds when compared to the parent $YBaCo_2O_{5.5}$ cobaltite. We have performed a structural characterization using neutron powder diffraction (NPD) to study the interplay between the structures and their magnetic order, and correlate this information with our previous magnetic studies.[27,28]

II. EXPERIMENTAL METHODS

Three polycrystalline samples were prepared by solid-state reaction. High-purity powders of Y_2O_3, $BaCO_3$, $CaCO_3$, and Co_3O_4 were mixed at stoichiometric weights to prepare the compounds $YBaCo_2O_{5.5}$ (x_{Ca}=0), $YBa_{0.95}Ca_{0.05}Co_2O_{5.5}$ (x_{Ca}=0.05), and $YBa_{0.90}Ca_{0.10}Co_2O_{5.5}$ (x_{Ca}=0.10). After a decarbonation process at 1173 K for 18 h, the mixtures were pressed into pellets and annealed. The samples were annealed together during 25 h at 1273 K and slowly cooled at 1 K/min in oxygen flow. After a regrinding of the resulting pellets, the compression and annealing at 1273 K in oxygen processes were repeated. A single batch was used for all the samples to guarantee identical synthesis conditions, which resulted in samples of about 1.5 g.

The oxygen content in our samples has been determined by refinement of our NPD data. In addition, we have compared the macroscopic magnetization and resistivity of our x_{Ca}=0 sample with a very detailed study of the parent compound $YBaCo_2O_{5+\delta}$ early reported by Akahoshi and Ueda.[29] Their work presents the existing correlation between oxygen content and magnetic and transport properties. In particular, the magnetization curve for our sample (Fig. 5) reveals an excellent quantitative agreement with their results for δ=0.5 and a clear disagreement outside the range $0.44<\delta\leqslant 0.52$. Moreover, the resistivity measurements in our samples[28] show the characteristic sharp jump of the MI transition, which has been shown to occur only for $0.45<\delta\leqslant 0.65$ but only to be sharp for $\delta\simeq 0.5$.[4] These limits give us confidence in the refined values from our NDP data. The global oxygen contents refined independently from eight high-resolution diffractograms, corresponding to different samples and temperatures—always below 350 K—were in mutual agreement within experimental error, yielding an average value of $\delta=0.46\pm0.02$. In the following we shall refer to the samples using the notation $Y(Ba,Ca)Co_2O_{5.5}$.

Neutron thermodiffraction data were collected on the high-intensity two-axis diffractometer D20 located at the High Flux Reactor of Institute Laue-Langevin ILL, Grenoble, France. Samples with x_{Ca}=0.05 and x_{Ca}=0.10 were cooled in a standard orange cryostat from room temperature down to 20 K, and diffraction patterns were then collected every 2 min at a warming rate of 1 K/min from 20 K to 320 K. A wavelength of ~2.41 Å was used to high-

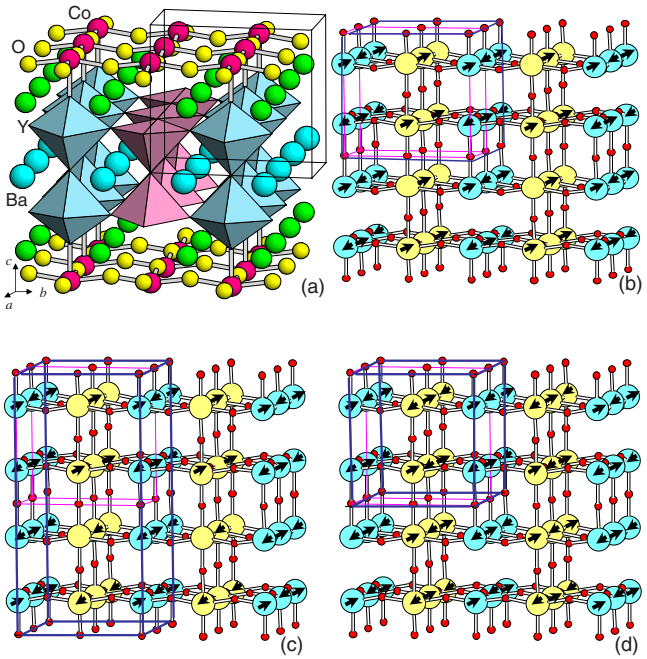

FIG. 1. (Color online) (a) The structure of $YBaCo_2O_{5.5}$. Half of the Co atoms are in square-pyramidal coordination and the other half in octahedral coordination. (b) Magnetic model adopted for the SSO ferrimagnetic phase after Ref. 17. The nuclear "122" unit cell and the magnetic "222" unit cell are indicated, and light atoms correspond to octahedral coordination. In this schematic representation, only Co and O atoms are shown for clarity. (c) Magnetic model adopted for the AFM-$O2$ phase after Ref. 17. (d) Magnetic model adopted for the AFM-$O1$ phase.

light the magnetic diffraction and was calibrated using a silicon sample.

In addition, high-resolution NPD data were collected at diffractometer Super-D2B of ILL for samples with $x_{Ca}=0$, 0.05, and 0.10. A wavelength of ~1.594 Å was used to collect patterns at selected temperatures for approximately 3 h. It is worth noting that the volume of sample available was not as much as the ideal for this kind of experiment, so we looked for a compromise between the collection time, the available beam time, and our capabilities for preparing all the samples in a single batch. The NPD patterns were processed with the full-pattern analysis Rietveld method, using the program FULLPROF (Ref. 30) for refining the crystal and magnetic structures.

III. RESULTS

A. Description of structures and refinement strategy

The room-temperature structures of the parent compound $YBaCo_2O_{5+\delta}$ were first reported by Akahoshi and Ueda,[29] who showed that for $\delta=0.5$ there may form two competing structures. One of them is orthorhombic and corresponds to the space group $Pmmm$ having the "122" superstructure characteristic of similar cobaltites with $\delta=0.5$.[2,3,7,23] A schematic representation of this phase is shown in Fig. 1. The vacancies order consists of alternating $[CoO_6]$ octahedra chains along the c axis and corner-sharing $[CoO_5]$ pyramids along the b axis, resulting in alternating octahedral and pyramidal layers in the a-c plane. This produces a doubling of the cell along the b axis, with a unit cell $a_P \times 2a_P \times 2a_P$. The second structure that may stabilize in this system for $\delta=0.5$ (and other values as well) has a tetragonal symmetry and no doubling of the b axis—i.e., no ordering between pyramids and octahedra. In this case, the space group is $P4/mmm$ and the unit cell $a_P \times a_P \times 2a_P$. Recently, Frontera *et al.*[6] have shown that, although the order of vacancies may not always be perfectly achieved, the order between the R-cation layer and the Ba layer is well established and there is no mixing between them. Nor are there significant oxygen vacancies in the [BaO] layers. The "122" structure admits a certain degree of disorder, consisting of misplaced pyramids or octahedra, but keeping the long-range "122″ order.

In the present refinements, the Ca cations were randomly introduced in the structure at the crystallographic site occupied by Ba in appropriate proportions. We have found no evidence of Ca segregation or the formation of additional phases, so we believe that Ca has been successfully incorporated into the cobaltite structure. The strategy for the Rietveld refinement was as follows. First, the high-resolution data from D2B were refined to obtain an accurate nuclear structure for each sample. The raw data coming from the Super-D2B detector were processed using the LAMP software[31] to obtain two sets of data: one of them having a better angle resolution at the expense of losing some neutron counts, the other one having all neutron counts collapsed into a single diffractogram. The first set was used to determine the lattice parameters, while the second set was used to refine the atomic positions and temperature factors, and both sets were iteratively refined until convergence to the structure. The magnetic structures were also included in the refinements. The models we have used will be discussed in the following sections. At a second step, the structural data obtained were used to refine sequentially the neutron thermodiffractograms obtained at D20. Temperature scans where divided into different ranges according to the structural and magnetic order, and for each range the atomic positions and occupations obtained at D2B were kept fixed, while lattice parameters, temperature factors, and magnetic moments were allowed to vary.

The objective of this work is to focus on the role of Ca addition to the parent compound $YBaCo_2O_{5.5}$. Our results will show that there is a clear logical sequence between the three samples studied, corresponding to $x_{Ca}=0$, $x_{Ca}=0.05$, and $x_{Ca}=0.10$. Surprisingly, the sample with greater Ca content, $x_{Ca}=0.10$, turned out to be the simplest one, and as Ca is removed, the complexity increases, resulting in a quite complicated temperature evolution of the parent compound. This fact probably explains why this compound has not yet been fully reported in such detail as other R cobaltites, except for the structural study by Akahoshi and Ueda[8] and a recent neutron diffraction study by Khalyavin *et al.*[32] focusing on the ferrimagnetic to paramagnetic transition. For the above reasons, we will present our results following the decreasing Ca sequence.

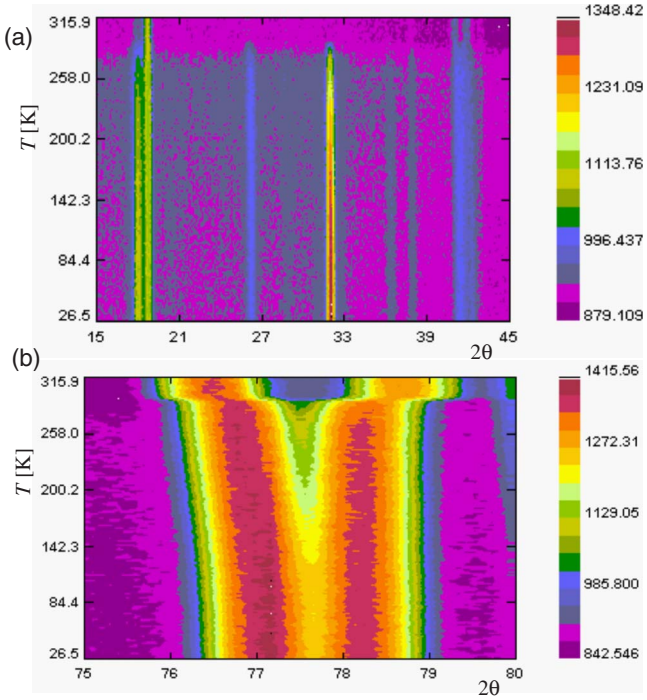

FIG. 2. (Color online) Projection of two selected sections of the thermodiffractograms corresponding to the sample x_{Ca}=0.10. (a) $16° < 2\theta < 44°$ and (b) $75° < 2\theta < 80°$ showing the (2 0 0) and (0 4 0) Bragg reflections of the "122" structure. Data were collected at D20 with $\lambda \sim 2.41$ Å between 20 K and 320 K.

B. Sample with x_{Ca}=0.10

In Fig. 2 we present two different sections of the projected thermodiffractograms for the sample x_{Ca}=0.10. Figure 2(a) corresponds to the low-angle range, in which most reflections are of magnetic nature and disappear simultaneously at ~295 K on warming from 20 K to 300 K. In Fig. 2(b) we focus on the 2θ range where the Bragg reflections (2 0 0) and (0 4 0) clearly show a distortion occurring at room temperature.

The high-resolution data were refined using a nuclear phase with the "122" structure, as described in Sec. III A. We do not discard the possibility of the actual structure being "222," with a doubling of the *a* axis and four different crystallographic sites for the Co atoms,[17,32] in line with the magnetic model adopted. However, as we are interested in the temperature evolution of rather low-resolution data from D20 and given the complexity of the other samples, we have decided to refine the whole series with the averaged "122" structure. Moreover, following Frontera *et al.*[11] we have fixed the *z* coordinate of the octahedral Co site to 1/4 in order to obtain centrosymmetric octahedra. With these assumptions, we reduced the number of free parameters, which is critical when dealing with multiphasic systems. We have nevertheless allowed for disorder between pyramids and octahedra by refining the occupation of apical oxygen sites (site 1*g* mostly occupied and site 1*c* mostly unoccupied in the *Pmmm* space group). We remark that even for different degrees of vacancies disorder, the total occupation of sites always summed up to the same oxygen content in all samples below 350 K. In Table I we present the details of the refined structure for the sample with x_{Ca}=0.10 from D2B data collected at 70 K, 230 K, and 348 K.

TABLE I. Structural parameters refined from the high-resolution D2B data for the compound $YBa_{0.90}Ca_{0.10}Co_2O_{5.5}$ at T=70 K, 230 K, and 350 K. Atomic fractional coordinates correspond to space group *Pmmm* in the following Wyckoff positions: Y $(2p)=(0.5,y,0.5)$; Ba, Ca $(2o)=(0.5,y,0)$; CoOct $(2r)=(0,0.5,0.25)$; CoPyr $(2q)=(0,0,z)$; O1 $(1a)=(0,0,0)$); O2 $(1e)=(0,0.5,0)$; O3 $(1g)=(0,0.5,0.5)$; O3′ $(1c)=(0,0,0.5)$; O4 $(2s)=(0.5,0,z)$; O5 $(2t)=(0.5,0.5,z)$; O6 $(4u)=(0,y,z)$.

		T=70 K	T=230 K	T=350 K
Y	*y*	0.2714(5)	0.2717(5)	0.2684(5)
Ba, Ca	*y*	0.253(1)	0.254(1)	0.248(1)
CoPyr	*z*	0.260(1)	0.260(1)	0.262(1)
O4	*z*	0.3112(7)	0.3108(7)	0.3107(7)
O5	*z*	0.276(1)	0.276(1)	0.271(1)
O6	*y*	0.2481(8)	0.2479(8)	0.2416(8)
O6	*z*	0.2954(6)	0.2947(5)	0.2980(5)
O3	*Occ*	0.94(2)	0.93(2)	0.89(2)
O3′	*Occ*	0.0	0.0	0.02(2)
a (Å)		3.8423(1)	3.8438(1)	3.8254(1)
b (Å)		7.7947(2)	7.8118(2)	7.8503(2)
c (Å)		7.4835(2)	7.4965(2)	7.5217(2)
R_B		7.4	7.4	7.1
R_{mag}		13.6	14.7	
χ^2		7.4	5.8	5.2

The model we have adopted for refining the magnetic phase is the SSO ferrimagnetic model proposed by Khalyavin *et al.*,[17,32] which leads to the best agreement with our NPD data, macroscopic magnetization data, and high-temperature susceptibility data.[27,28] It is schematized in Fig. 1(b). Although the model involves Co atoms at half the octahedral sites being in the low-spin state, and therefore having a magnetic moment equal to zero, after a first step in the refinement we allowed this site to adopt a nonzero magnetic moment, which resulted in a small value compatible with the fact that the apical oxygen site 1*g* is not completely occupied, and therefore some octahedra are, in fact, misplaced pyramids.[11] In Fig. 3(a) we present the evolution with temperature of the lattice parameters refined in the *Pmmm* "122" structure. The sequential D20 results are presented together with the results from D2B at the studied temperatures. The characteristic structural distortion occurring at $T_{MI} \sim 295$ K is clearly observed. We have already reported that in this system, the MI transition occurs almost simultaneously with the paramagnetic-ferrimagnetic transition,[27] which seems to be only a coincidence. Therefore, no further anomaly is observed in the lattice parameters down to 20 K, as there is in this sample no further magnetic transition. In Fig. 4(a) we present the magnetic moment of Co atoms in each crystallographic environment. We have not included in the figure the small magnetic moment of misplaced pyramids, which remains always less than $0.4\mu_B$.

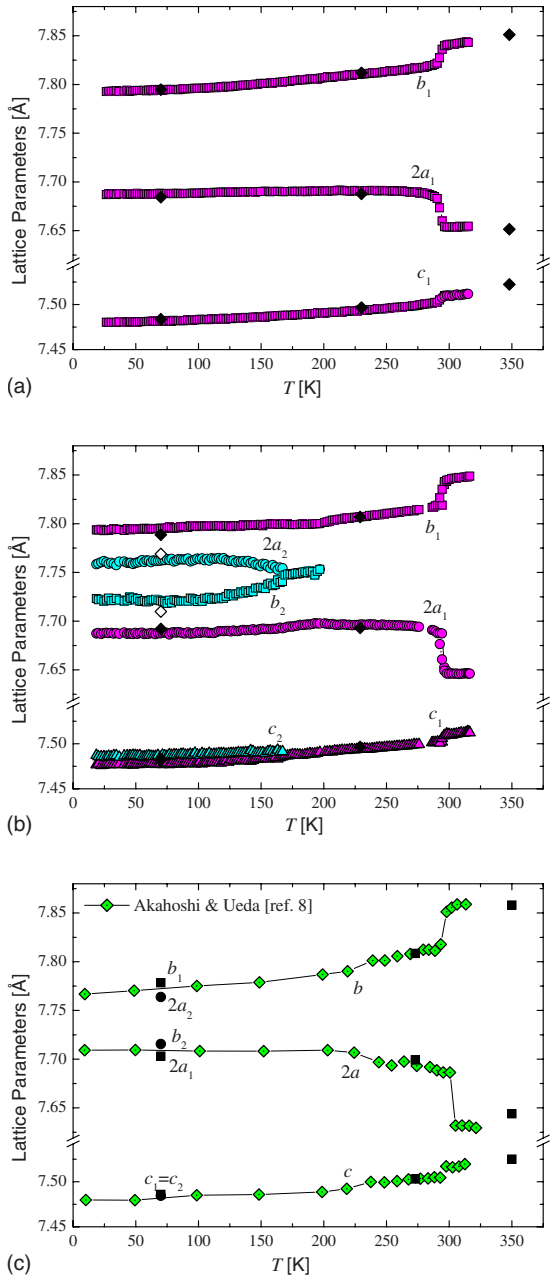

FIG. 3. (Color online) Thermal evolution of the lattice parameters $2a$, b, and c for the $O1$ (dark symbols) and $O2$ (light symbols) phases in samples with $x_{Ca}=0.10$ (a), $x_{Ca}=0.05$ (b), and $x_{Ca}=0$ (c), determined from data collected at D20 and D2B. In (c) the data from D2B (solid symbols) are compared with data reported by Akahoshi and Ueda (Ref. 8), plotted using diamonds.

C. Sample with $x_{Ca}=0.05$

Our preliminary x-ray diffraction pattern of the as-synthesized sample $x_{Ca}=0.05$ at room temperature resulted in being identical to $x_{Ca}=0.10$ with just a slight difference in the lattice parameters, indicating that the room-temperature structure is the same in both samples. However, the macroscopic magnetization data in Fig. 5 show that at low temperature they behave differently. Below 200 K, on cooling, the magnetization of the $x_{Ca}=0.05$ sample starts dropping but

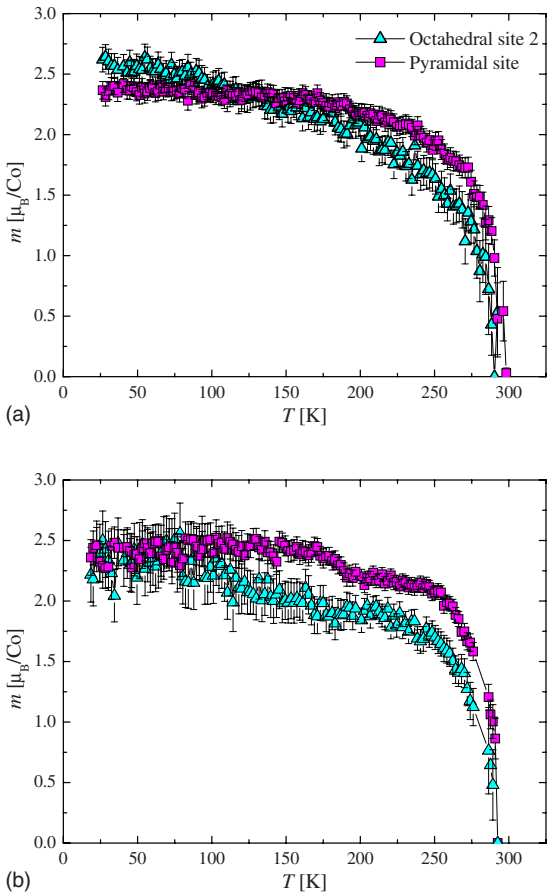

FIG. 4. (Color online) Temperature dependence of the magnetic moments in pyramids (square symbols) and half the octahedra (triangular symbols) for the samples $x_{Ca}=0.10$ (a) and $x_{Ca}=0.05$ (b), obtained from the Rietveld refinements of neutron data collected at D20. Moments were refined along [100].

the sample retains a net magnetization down to 5 K, in contrast with the parent compound $x_{Ca}=0$ which shows an AFM behavior. Moreover, the large hysteresis between the data collected on cooling and warming in the $x_{Ca}=0.05$ sample suggests that there is competition between two states. The NPD experiments reveal the nature of these two states.

In Fig. 6(c) we present a projection of the thermodiffractograms collected at D20 for sample $x_{Ca}=0.05$. In (a) and (b) we show the temperature evolution of the intensity of the magnetic reflections (0 1 0) and (1/2 1 1), respectively, indexed in terms of the "122" nuclear phase. These reflections correspond to the ferrimagnetic order discussed in the previous subsection. Figures 6(a) and 6(b) compare the intensities of these reflections in samples $x_{Ca}=0.05$ and $x_{Ca}=0.10$. We can observe that they both behave almost identically from 200 K to 320 K, but below 200 K the ferrimagnetic reflections are lower in the $x_{Ca}=0.05$ sample. Moreover, at 200 K additional features are evidenced in the thermodiffractograms. The small arrows in Fig. 6(c) mark two reflections which appear only below 200 K. They are indicative of the presence of a second—magnetically ordered—phase which may be indexed with a further doubling of the c parameter as reported by various authors in the AFM region of layered

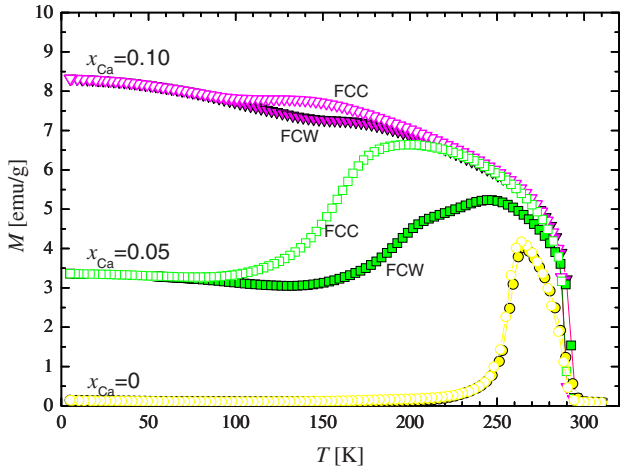

FIG. 5. (Color online) Low-field magnetization as a function of temperature for samples with $x_{Ca}=0$, $x_{Ca}=0.05$, and $x_{Ca}=0.10$. Open symbols represent the magnetization measured on cooling under a magnetic field of 5 kOe (FCC), and solid symbols represent the magnetization subsequently measured on warming (FCW).

cobaltites.[11,15–17,19] But here we also observe simultaneous changes in the nuclear structure, and not only a magnetic phase separation or gradual magnetic transition to a different magnetic arrangement.[11,15,16] This is illustrated, for instance, by a peak arising at 200 K in $2\theta \sim 77.6°$ lying in between the (2 0 0) and (0 4 0) reflections of the "122" nuclear phase. In Fig. 7 we show the evolution with temperature of the collected intensity at $2\theta \sim 77.6°$ for this sample as well as for the sample with $x_{Ca}=0.10$ for comparison. When warming, there is a sudden drop at 200 K to a value corresponding to the overlap of the neighboring (2 0 0) and (0 4 0) reflections and a further drop to background values above the MI transition when these reflections are suddenly shifted apart by the distortion. We first evaluated the possibility of this behavior being a result of a distortion of the "122" nuclear phase at 200 K. Such a hypothesis gave no satisfactory results when trying to refine simultaneously the D2B and D20 data at 70 K. Additional attempts to model the $70° < 2\theta < 80°$ region using Gaussian peaks of just one orthorhombic phase, even allowing for unrealistically wide peaks, could not reproduce the triple-peak shape observed in the D20 spectra (inset in Fig. 7).

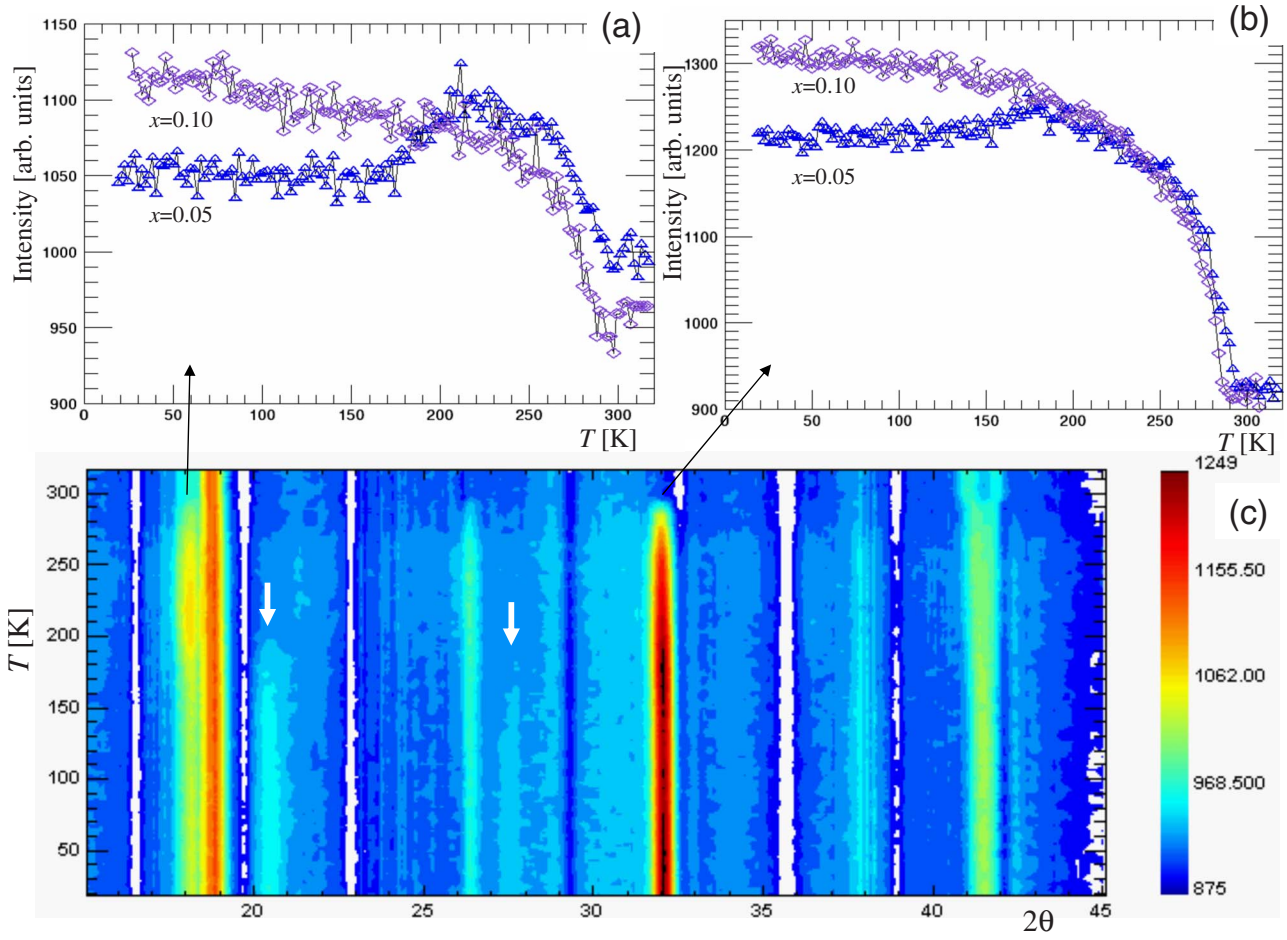

FIG. 6. (Color online) Thermal evolution of the intensity of Bragg reflections (0 1 0) (a) and (1/2 1 1) (b) indexed in terms of the "122" phase for samples with $x_{Ca}=0.05$ (triangles) and $x_{Ca}=0.10$ (diamonds) from data collected at D20. (c) Two-dimensional projection of the neutron thermodiffractograms collected at D20 for sample $x_{Ca}=0.05$ in the range $16° < 2\theta < 44°$. The small arrows indicate the onset of magnetic reflections from the AFM "224" phase. The long arrows between graphs indicate the position in the thermodiffractogram of the two reflections whose intensity is plotted in (a) and (b).

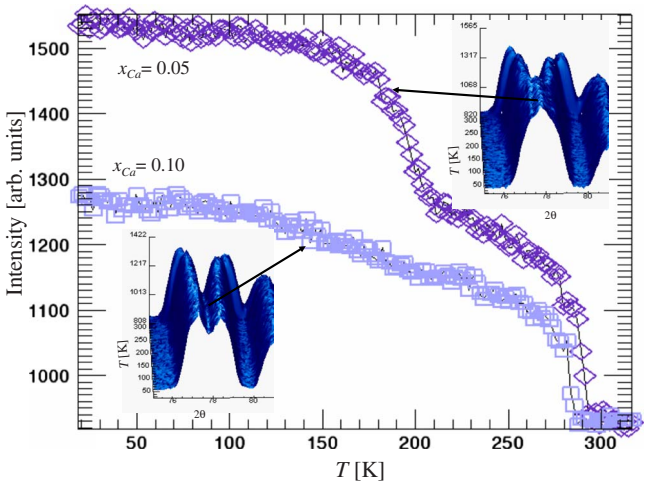

FIG. 7. (Color online) Thermal evolution of the intensity in the thermodiffractograms at $2\theta \sim 77.6°$ in the position between the (2 0 0) and (0 4 0) Bragg reflections of the "122" phase for the sample with $x_{Ca}=0.05$ (diamonds) and $x_{Ca}=0.10$ (squares). The insets show the three-dimensional thermodiffractograms for the relevant 2θ range.

We also considered other structural models to account for the low-temperature data coming from D2B and D20. Neither the *Pcca* nor *Pmma* space groups proposed by Plakhty *et al.*[15] and Khalyavin *et al.*,[32] together with the respective magnetic models proposed in their work, gave satisfactory results for the simultaneous refinement of all our data.

Another possible explanation is the presence of a second structural phase. This is suggested by the poor results obtained refining the D2B data using the same (single-phase) model as for the $x_{Ca}=0.10$ sample at 70 K (*Pmmm* space group), as well as with other single-phase models (*Pcca*, *Pmma*). Based on the D20 data, we considered a possible second phase with a strong tetragonal distortion, which would not be unreasonable considering that a two-phase mixture of orthorhombic and tetragonal phases for $YBaCo_2O_{5.5}$ had already been reported by Akahoshi and Ueda,[29] both phases occurring competitively. It is also worth noting that in the same batch as the present samples, we have also synthesized a series of samples where barium is replaced by strontium, a substitution which clearly favors a tetragonal phase in which the position of the (2 0 0) Bragg reflection is almost exactly coincident with this new peak in the $x_{Ca}=0.05$ sample.[33] Consequently, we tried to refine both the D2B and D20 sets of data using a mixture of the "122" phase and a tetragonal ($P4/mmm$) phase. This gave no satisfactory results either, and moreover, the proposed tetragonal symmetry could not account for the observed magnetic supercell.

We finally proceeded to adopt for the second phase an orthorhombic (*Pmmm*) cell with the constraint $b=2a$, and at a further step we allowed the b and a lattice parameters to vary independently. The diffractogram at 70 K was therefore refined with one orthorhombic phase with ferrimagnetic order ($O1$ phase) plus a second orthorhombic phase ($O2$) with AFM order which is consistent with a "224" supercell. This finally gave much more satisfactory results for the refinement. The magnetic peaks arising below 200 K, although weak, could be accounted for using the AFM model proposed by Khalyavin,[17] schematized in Fig. 1(c), with the constraint of a single magnitude for the magnetic moment of all Co atoms in pyramidal positions and, once again (as in the ferrimagnetic SSO model), two possible spins for octahedral Co. At 230 K, the $O1$ phase with ferrimagnetic order was enough to refine the D2B diffractogram. In Table II we present the details of the refined structures for the sample with $x_{Ca}=0.05$ from D2B data collected at 70 K and 230 K. Figure 8 shows the Rietveld refinement (solid line) of the high-resolution data (symbols) collected at 70 K. The four sets of Bragg reflections indicated at the bottom by vertical bars correspond to each of the above-mentioned phases. The difference pattern between observed and calculated data is also shown.

TABLE II. Structural parameters refined from the high-resolution D2B data for the compound $YBa_{0.95}Ca_{0.05}Co_2O_{5.5}$ at $T=70$K and 230 K. Two sets of atomic fractional coordinates are given for the $O1$ and $O2$ phases, which correspond to space group *Pmmm* in the following Wyckoff positions: Y $(2p)=(0.5,y,0.5)$; Ba, Ca $(2o)=(0.5,y,0)$; CoOct $(2r)=(0,0.5,0.25)$; CoPyr $(2q)=(0,0,z)$; O1 $(1a)=(0,0,0)$); O2 $(1e)=(0,0.5,0)$; O3 $(1g)=(0,0.5,0.5)$; O3′ $(1c)=(0,0,0.5)$; O4 $(2s)=(0.5,0,z)$; O5 $(2t)=(0.5,0.5,z)$; O6 $(4u)=(0,y,z)$.

		$T=70$ K		$T=230$K
		$O1$	$O2$	$O1$
Y	y	0.2757(8)	0.264(2)	0.2731(5)
Ba, Ca	y	0.254(1)	0.233(3)	0.254(1)
CoPyr	z	0.262(2)	0.267(2)	0.261(1)
O4	z	0.317(1)	0.291(5)	0.3125(7)
O5	z	0.261(2)	0.287(5)	0.274(1)
O6	y	0.2460(9)	0.243(2)	0.2473(7)
O6	z	0.2941(6)	0.301(1)	0.296(1)
O3	Occ	1.0	0.84(6)	0.92(2)
O3′	Occ	0.0	0.0	0.00(2)
a (Å)		3.8460(2)	3.8845(3)	3.8468(1)
b (Å)		7.7887(4)	7.7099(6)	7.8075(2)
c (Å)		7.4827(5)	7.4819(7)	7.4959(2)
f (%)		64(4)	36(3)	100
R_B		7.0	7.0	7.3
R_{mag}		15	32	16
χ^2				4.48

The presented scenario for the evolution with temperature of the $x_{Ca}=0.05$ sample yields consistent results among the D2B and D20 data, as well as it accounts for other experimental facts. When cooling from room temperature, the intensity of the ferrimagnetic reflections starts dropping because there is a second phase developing in the sample, so that the volume fraction of the ferrimagnetic phase is reduced. In addition, the observed hysteresis among the FCC and FCW magnetization curves in Fig. 5 is also indicative of a possible phase separation, as well as the hysteresis in the

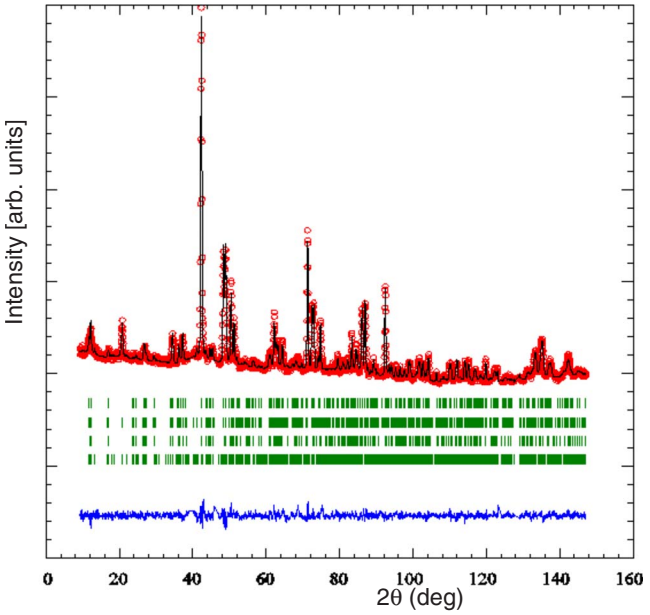

FIG. 8. (Color online) Rietveld refinement for the sample with $x_{Ca}=0.05$ from data collected at D2B at $T=70$ K. Vertical bars at the bottom indicate Bragg reflections from the phases included in the refinement: the nuclear phases $O1$ and $O2$ and the magnetic phases SSO "222" and AFM "224."

resistivity curves presented previously.[28] The presence of a second nuclear phase has become more evident when performing thermodiffractograms with $\lambda=2.52$ Å. This scenario would be very difficult to infer just from D2B data collected at lower wavelengths and at isolated temperatures, due to peak overlap and to a lack of perspective of the continuous thermal evolution of the sample.

The evolution with temperature of the lattice parameters refined in the $O1$ and $O2$ phases is shown in Fig. 3(b). The sequential D20 results are presented together with the results from D2B at the studied temperatures. For the $O1$ phase, the distortion at $T_{MI}\sim 295$ K is again observed as in the sample with $x_{Ca}=0.10$. For the $O2$ phase, we observe a tetragonal distortion above 170 K: above that temperature the a_2 and b_2 lattice parameters could only be refined using the constraint $2a_2=b_2$. The volume per atom of both phases is practically the same, although it is observed that the lattice parameter relation is different ($2a_1<b_1, 2a_2>b2$). It would be interesting to stabilize the $O2$ phase to get more detailed information of its structural properties.[33] In Fig. 4(b) we present the magnetic moment of Co atoms in the ferrimagnetic phase for each crystallographic environment. We have not included in the figure the small magnetic moment of misplaced pyramids, which remains always less than $0.5\mu_B$. Unfortunately, the quality of our D20 data and the two-phase scenario does not allow for a confident determination of the magnetic moments in the $O2$ AFM phase. These were constrained to be aligned along [100] following the model described above and to adopt values similar to those in the $O1$ phase in order to obtain reliable phase fractions which were comparable to the values refined from D2B data.

Figure 9 shows the net spontaneous magnetization of samples with $x_{Ca}=0.05$ and $x_{Ca}=0.10$, obtained as $M=\mu_{Co}f_{O1}$, where μ_{Co} represents the net magnetic moment per Co atom in the ferrimagnetic phase ($=\mu_{CoOct}/4$) and f_{O1} is the refined phase fraction of the $O1$ phase. These results can be compared with the macroscopic determination of the magnetization of the samples as a function of temperature (Fig. 5), always considering these were collected under an applied field of 5 kOe. The overall similarity between the curves is in excellent agreement.

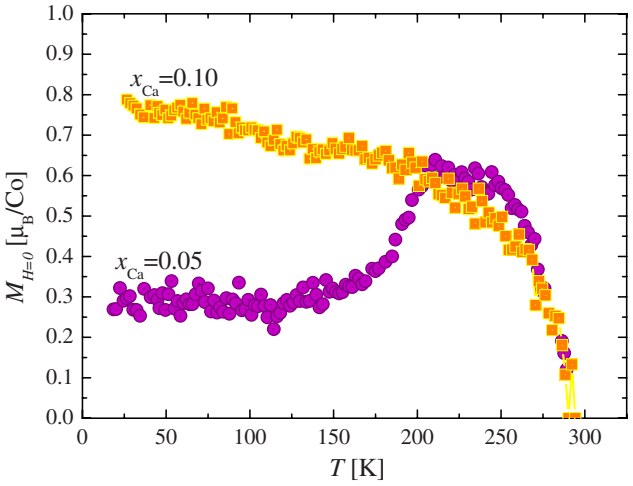

FIG. 9. (Color online) Spontaneous magnetization of the ferrimagnetic phase in samples with $x_{Ca}=0.05$ and $x_{Ca}=0.10$, obtained from our NPD refinements as $M=\mu_{Co}f_{O1}$, where μ_{Co} represents the net magnetic moment per Co atom ($=\mu_{CoOct}/4$) and f_{O1} is the phase fraction of the $O1$ phase.

D. Sample with $x_{Ca}=0$

We finally turn to the parent compound. This sample was only studied in the high-resolution instrument, so we cannot present continuous temperature scans in the low-temperature range as in the other samples. We collected three diffractograms at $T=70$ K, 273 K, and 348 K. A similar study on this system, very recently reported,[32] focused on the paramagnetic to ferrimagnetic transition, and very good agreement is found. It should be emphasized that those authors have refined the patterns using the expanded "222" cell for the nuclear phase in the ferrimagnetic region in the *Pmma* space group, a hypothesis which—as we mentioned before—we do not discard but prefer to use the "122" *Pmmm* cell to be consistent along the whole series. For the lowest temperature, however, those authors did not present any refinement of their data. The intriguing fact that the "222" magnetic reflections reappeared at 190 K after having disappeared at 265 K was left unexplained. In the present work, we show that our diffractogram at 70 K can be satisfactorily refined in the framework of the analysis presented for the $x_{Ca}=0.05$ sample. Therefore, the nuclear diffraction was accounted for by using two orthorhombic phases $O1$ and $O2$, and the whole set of magnetic reflections could then be assigned to each of these phases. As in $x_{Ca}=0.05$, the $O2$ phase presents an AFM ordering with a "224" magnetic cell. The $O1$ phase, on the other hand, cannot keep its ferrimagnetic SSO order because

TABLE III. Structural parameters refined from the high-resolution D2B data for the parent compound $YBaCo_2O_{5.5}$ at $T=70$ K, 273 K, and 348 K. Two sets of atomic fractional coordinates are given for the $O1$ and $O2$ phases, which correspond to space group *Pmmm* in the following Wyckoff positions: Y $(2p)=(0.5,y,0.5)$; Ba, Ca $(2o)=(0.5,y,0)$; CoOct $(2r)=(0,0.5,0.25)$; CoPyr $(2q)=(0,0,z)$; O1 $(1a)=(0,0,0)$); O2 $(1e)=(0,0.5,0)$; O3 $(1g)=(0,0.5,0.5)$; O3′ $(1c)=(0,0,0.5)$; O4 $(2s)=(0.5,0,z)$; O5 $(2t)=(0.5,0.5,z)$; O6 $(4u)=(0,y,z)$.

		$T=70$ K		$T=273$ K	$T=348$ K
		$O1$	$O2$	$O1$	$O1$
Y	y	0.2809(9)	0.271(1)	0.2745(6)	0.2692(5)
Ba	y	0.255(2)	0.238(2)	0.254(1)	0.244(1)
CoP	z	0.251(3)	0.270(3)	0.261(1)	0.260(1)
O4	z	0.321(2)	0.300(2)	0.3127(9)	0.3126(7)
O5	z	0.251(2)	0.276(3)	0.274(1)	0.267(1)
O6	y	0.2449(9)	0.243(1)	0.2495(9)	0.2437(8)
O6	z	0.299(1)	0.300(1)	0.2935(7)	0.2984(5)
O3	Occ	1.0	0.67(6)	0.86(3)	0.81(2)
O3′	Occ	0.0	0.18(4)	0.05(2)	0.12(2)
a (Å)		3.8515(2)	3.8819(2)	3.8496(1)	3.8221(1)
b (Å)		7.7785(5)	7.7156(4)	7.8085(2)	7.8581(3)
c (Å)		7.4859(6)	7.4845(6)	7.5032(2)	7.5250(2)
f (%)		42(3)	58(3)	100	100
R_B		7.7	7.5	8.1	6.4
χ^2		3.98		3.97	3.53

this would not be compatible with the macroscopic magnetization measurements. In addition, a close inspection of the magnetic peaks reveals that not all the reflections from the 273 K ferrimagnetic phase are present, but that contributions to intensity related to FM planes are absent at 70 K. Therefore, we have used a second AFM model for the $O1$ phase at 70 K, with a "222" magnetic cell and a G-type ordering, although we have allowed for different magnetic moment values in pyramids and octahedra. The model is schematized in Fig. 1(d). This scenario is also supported by our data on a different sample, substituted with 5% Sr $[Y(Ba_{0.95}Sr_{0.05})Co_2O_{5.5}]$ for which we have also performed neutron thermodiffraction scans and apparently behaves almost the same as the parent compound. These results will be published in a separate paper.[33]

In Table III we present the details of the refined structures for the sample with $x_{Ca}=0$ from D2B data. The diffractogram at 70 K was refined with the $O1+O2$ mixture, plus two AFM phases associated with each of them, one having a "224" supercell and the other one with a "222" supercell. At 230 K, only the $O1$ phase with ferrimagnetic order was enough to refine the diffractogram, whereas at 348 K just the nuclear $O1$ phase was refined. It is worth noting that the parent compound seems to have a higher degree of misplaced octahedra when compared to the Ca-substituted samples. This is evidenced by the nonzero occupation of the O3′ site, which corresponds to the empty apical oxygen position of pyramids. At the highest temperature, however, there is a slight rearrangement of vacancies among the O3 and O3′ sites. When comparing the low-temperature phases $O1$ and $O2$ in the $x_{Ca}=0$ and $x_{Ca}=0.05$ samples, we observe that the $O1$ phase seems to prefer a more perfect order of pyramids and octahedra, while the excess oxygen vacancies accommodate in the $O2$ phase. There is also consistency among the structural parameters in both samples for the $O1$ and $O2$ phases. The results for the refined lattice parameters at the three temperatures studied are shown in Fig. 3(c). Our data are compared with those published by Akahoshi and Ueda (diamonds).[29] The difference at 70 K is due to the use of one or two phases to refine the data. We have found no way of indexing the whole set of magnetic reflections based on a single nuclear structure. It has been shown in other *R* cobaltites that there could be two coexisting magnetic arrangements on a single nuclear structure.[11–16] However, the evidence found in the $x_{Ca}=0.05$ thermodiffractograms and the consistency obtained in the whole series when adopting such a phase separation model give us confidence in the proposed scenario. The complexity of the systems seems to be related to the small size of the *R* cation.

IV. CONCLUDING REMARKS

Although the layered cobaltites $RBaCo_2O_{5.5}$ have received great attention in the past five years, much of its behavior remains still controversial and unclear. In this paper, an attempt is made to get some insight into the role of cationic disorder by substituting the Ba site, a topic that has not yet been investigated to the best of our knowledge. Interestingly, the systematics of this substitution led us to clarify and to propose a model that describes the behavior at low temperature of the undoped parent compound. Even though Ca addition does not lead to severe structural distortions, it has nevertheless dramatic effects on the magnetic arrangement and stability of the ferrimagnetic phase on detriment of the AFM long-range order. Our results open up the possibility of studying Ca-doped cobaltites in order to isolate the intrinsic properties of the "122" ferrimagnetic phase in monophasic samples, avoiding spurious effects in the analysis of macroscopic properties. Further work is in progress to investigate the role of different cations substitution and the systematics of the Ba-site disorder effects.

ACKNOWLEDGMENTS

This work is part of a research project supported by Agencia Nacional de Promoción Científica y Tecnológica (Argentina), under Grants Nos. PICT 17-21372 and 20144, by CONICET (Argentina) under Grants Nos. PIP 5250/05 and 5657/05, and by SECTyP, Universidad Nacional de Cuyo. J.C. acknowledges a grant from CNEA and CONICET. We particularly acknowledge ILL and its staff for the beam time allocation and technical assistance.

*Corresponding author. Also at CIC, Consejo Nacional de Investigaciones Científican y Técnicas. gaurelio@cab.cnea.gov.ar
†Also at Instituto Balseiro, Universidad Nacional de Cuyo.
‡Also at CIC, Consejo Nacional de Investigaciones Científicas y Técnicas. Also at Instituto Balseiro, Universidad Nacional de Cuyo.

[1] C. Martin, A. Maignan, D. Pelloquin, N. Nguyen, and B. Raveau, Appl. Phys. Lett. **71**, 1421 (1997).
[2] M. Respaud, C. Frontera, J. L. García-Muñoz, M. A. G. Aranda, B. Raquet, J. M. Broto, H. Rakoto, M. Goiran, A. Llobet, and J. Rodríguez-Carvajal, Phys. Rev. B **64**, 214401 (2001).
[3] D. D. Khalyavin, S. N. Barilo, S. V. Shiryaev, G. L. Bychkov, I. O. Troyanchuk, A. Furrer, P. Allenspach, H. Szymczak, and R. Szymczak, Phys. Rev. B **67**, 214421 (2003).
[4] A. A. Taskin, A. N. Lavrov, and Y. Ando, Phys. Rev. B **71**, 134414 (2005).
[5] Z. X. Zhou and P. Schlottmann, Phys. Rev. B **71**, 174401 (2005).
[6] C. Frontera, A. Caneiro, A. E. Carrillo, J. Oró-Solé, and J. L. García-Muñoz, Chem. Mater. **17**, 5439 (2005).
[7] Y. Moritomo, T. Akimoto, M. Takeo, A. Machida, E. Nishibori, M. Takata, M. Sakata, K. Ohoyama, and A. Nakamura, Phys. Rev. B **61**, R13325 (2000).
[8] D. Akahoshi and Y. Ueda, J. Solid State Chem. **156**, 355 (2001).
[9] A. Maignan, V. Caignaert, B. Raveau, D. Khomskii, and G. Sawatzky, Phys. Rev. Lett. **93**, 026401 (2004).
[10] C. Frontera, J. L. García-Muñoz, A. Llobet, and M. A. G. Aranda, Phys. Rev. B **65**, 180405(R) (2002).
[11] C. Frontera, J. L. García-Muñoz, A. E. Carrillo, M. A. G. Aranda, I. Margiolaki, and A. Caneiro, Phys. Rev. B **74**, 054406 (2006).
[12] C. Frontera, J. L. García-Muñoz, A. Llobet, Ll. Mañosa, and M. A. G. Aranda, J. Solid State Chem. **171**, 49 (2003).
[13] K. Takubo, J.-Y. Son, T. Mizokawa, M. Soda, and M. Sato, Phys. Rev. B **73**, 075102 (2006).
[14] E. Pomjakushina, K. Conder, and V. Pomjakushin, Phys. Rev. B **73**, 113105 (2006).
[15] V. P. Plakhty, Yu P. Chernenkov, S. N. Barilo, A. Podlesnyak, E. Pomjakushina, E. V. Moskvin, and S. V. Gavrilov, Phys. Rev. B **71**, 214407 (2005).
[16] F. Fauth, E. Suard, V. Caignaert, and I. Mirebeau, Phys. Rev. B **66**, 184421 (2002).
[17] D. D. Khalyavin, Phys. Rev. B **72**, 134408 (2005).
[18] D. L. Khomskii and U. Löw, Phys. Rev. B **69**, 184401 (2004).
[19] M. Soda, Y. Yasui, T. Fujita, T. Miyashita, M. Sato, and K. Kakurai, J. Phys. Soc. Jpn. **72**, 1729 (2003).
[20] M. Itoh, Y. Nawata, T. Kiyama, D. Akahoshi, N. Fujiwara, and Y. Ueda, Physica B **329-333**, 751 (2003).
[21] H. Kubo, K. Zenmyo, M. Itoh, N. Nakayama, T. Mizota, and Y. Ueda, J. Magn. Magn. Mater. **272-276**, 581 (2004).
[22] Yu. P. Chernenkov, V. P. Plakhty, V. I. Fedorov, S. N. Barilo, S. V. Shiryaev, and G. L. Bychkov, Phys. Rev. B **71**, 184105 (2005).
[23] H. Kusuya, A. Machida, Y. Moritomo, K. Kato, E. Nishibori, M. Takata, M. Sakata, and A. Nakamura, J. Phys. Soc. Jpn. **70**, 3577 (2001).
[24] M. Pouchard, A. Villesuzanne, and J. P. Doumerc, J. Solid State Chem. **162**, 282 (2001).
[25] V. Pardo and D. Baldomir, Phys. Rev. B **73**, 165117 (2006).
[26] Hua Wu, Phys. Rev. B **64**, 092413 (2001).
[27] G. Aurelio, J. Curiale, R. D. Sánchez, and R. E. Carbonio, Physica B **384**, 106 (2006).
[28] G. Aurelio, J. Curiale, R. D. Sánchez, and G. J. Cuello, Physica B **398**, 223 (2007).
[29] D. Akahoshi and Y. Ueda, J. Phys. Soc. Jpn. **68**, 736 (1999).
[30] J. Rodríguez-Carvajal, Computer code FULLPROF, a program for Rietveld refinement and pattern matching analysis, 1990.
[31] LAMP, the large array manipulation program, http://www.ill.fr/data_treat/lamp/front.html
[32] D. D. Khalyavin, D. N. Argyriou, U. Amann, A. A. Yaremchenko, and V. V. Kharton, Phys. Rev. B **75**, 134407 (2007).
[33] Aurelio *et al.* (unpublished).